Mon. Not. R. Astron. Soc. **352,** 153–167 (2004) doi:10.1111/j.1365-2966.2004.07908.x

Photometry of Magellanic Cloud clusters with the Advanced Camera for Surveys – I. The old Large Magellanic Cloud clusters NGC 1928, 1939 and Reticulum

A. D. Mackey★ and G. F. Gilmore
Institute of Astronomy, University of Cambridge, Madingley Road, Cambridge CB3 0HA

Accepted 2004 April 6. Received 2004 April 2; in original form 2004 February 17

ABSTRACT

We present the results of photometric measurements from images of the Large Magellanic Cloud (LMC) globular clusters NGC 1928, 1939 and Reticulum taken with the Advanced Camera for Surveys on the *Hubble Space Telescope*. Exposures through the F555W and F814W filters result in high-accuracy colour–magnitude diagrams (CMDs) for these three clusters. This is the first time that CMDs for NGC 1928 and 1939 have been published. All three clusters possess CMDs with features indicating them to be >10 Gyr old, including main-sequence turn-offs at $V \sim 23$ and well-populated horizontal branches (HBs). We use the CMDs to obtain metallicity and reddening estimates for each cluster. NGC 1939 is a metal-poor cluster, with $[\mathrm{Fe/H}] = -2.10 \pm 0.19$, while NGC 1928 is significantly more metal rich, with $[\mathrm{Fe/H}] = -1.27 \pm 0.14$. The abundance of Reticulum is intermediate between the two, with $[\mathrm{Fe/H}] = -1.66 \pm 0.12$ – a measurement which matches well with previous estimates. All three clusters are moderately reddened, with values ranging from $E(V-I) = 0.07 \pm 0.02$ for Reticulum and $E(V-I) = 0.08 \pm 0.02$ for NGC 1928, to $E(V-I) = 0.16 \pm 0.03$ for NGC 1939. After correcting the CMDs for extinction we estimate the HB morphology of each cluster. NGC 1928 and 1939 possess HBs consisting almost exclusively of stars to the blue of the instability strip, with NGC 1928 in addition showing evidence for an extended blue HB. In contrast, Reticulum has an intermediate HB morphology, with stars across the instability strip. Using a variety of dating techniques we show that these three clusters are coeval with each other and the oldest Galactic and LMC globular clusters, to within ∼2 Gyr. The census of known old LMC globular clusters therefore now numbers 15 plus the unique, younger cluster ESO121−SC03. The NGC 1939 field contains another cluster in the line of sight, NGC 1938. A CMD for this object shows it to be less than ∼400 Myr old, and it is therefore unlikely to be physically associated with NGC 1939.

Key words: globular clusters: individual: NGC 1928 – globular clusters: individual: NGC 1938 – globular clusters: individual: NGC 1939 – globular clusters: individual: Reticulum – Magellanic Clouds – galaxies: star clusters.

1 INTRODUCTION

The Large and Small Magellanic Clouds (LMC and SMC) possess extensive systems of rich stellar clusters. These objects exhibit a much wider variety in age, structure, environment and mass than do Galactic clusters, and this, combined with their relatively close proximity, has rendered them central to a surprising number of fields of modern astrophysics – from star and cluster formation, and stellar evolution, to gravitational dynamics, galactic evolution and distance scale measurements. They are also vital probes and tracers of the chemical and dynamical evolution of the LMC and SMC themselves. It is therefore important to understand how their properties, and in particular their ages and abundances, are distributed.

It has long been known that the LMC, which contains the more numerous cluster system of the two clouds, houses a small subpopulation of extremely ancient objects. Although early studies revealed half a dozen LMC clusters to possess colour–magnitude diagrams (CMDs) with features similar to those of the Galactic globular clusters, it has only been since the advent of the *Hubble Space Telescope* (*HST*) that imaging resolution and sensitivity has been sufficiently high as to allow accurate CMDs suitable for relative age dating. A

★E-mail: dmackey@ast.cam.ac.uk

number of relatively recent studies have demonstrated that the number of LMC clusters coeval with each other and the oldest Galactic globular clusters is more than a dozen – NGC 1466, 2257 and Hodge 11 (e.g. Johnson et al. 1999); NGC 1754, 1835, 1898, 1916, 2005 and 2019 (e.g. Olsen et al. 1998); and NGC 1786, 1841 and 2210 (e.g. Brocato et al. 1996). Several published CMDs show the remote outer cluster Reticulum to be very old (Johnson et al. 1999; Marconi et al. 2002; Monelli et al. 2003) however, a full age analysis is yet to be published for this cluster. In addition there are two more clusters located in the LMC bar region – NGC 1928 and 1939 – which integrated spectroscopy suggests could be old (Dutra et al. 1999), but which are so compact and lie against such highly crowded LMC fields that it has not previously been possible to obtain accurate CMDs for them [see e.g. the search for old LMC clusters conducted by Geisler et al. (1997)]. The census of old LMC clusters is therefore still incomplete.

We have used the Advanced Camera for Surveys (ACS) on *HST* to obtain images of NGC 1928, 1939 and Reticulum as part of programme 9891 – a snapshot survey of 40 LMC and 40 SMC clusters. This programme is primarily designed to extend the detailed investigation of Mackey & Gilmore (2003a,b) concerning the structural evolution of Magellanic Cloud clusters. However, the ACS observations are of sufficient quality and resolution as to allow CMDs to be constructed for NGC 1928 and 1939 for the first time, as well as a high-quality CMD for Reticulum. In this paper, we present the results of these observations (Section 2) and the measured CMDs (Section 3). Abundances and reddenings are derived for each cluster, and it is demonstrated that NGC 1928 and 1939, along with Reticulum, are coeval with both well-studied Galactic globular clusters (such as M92, M3 and M5) and other old LMC objects (such as NGC 2257 and Hodge 11) (Section 4).

2 OBSERVATIONS AND DATA REDUCTION

The observations were taken during *HST* Cycle 12 using the ACS Wide Field Channel (WFC). As snapshot targets, the clusters were observed for only one orbit each. This allowed two exposures to be taken per cluster – one through the F555W filter and one through the F814W filter. Details of the individual exposures are listed in Table 1. Exposure durations were 330 s in F555W and 200 s in F814W.

The ACS WFC consists of a mosaic of two 2048 × 4096 SITe CCDs with a scale of ∼ 0.05 arcsec per pixel, and separated by a gap of ∼50 pixels. Each image therefore covers a field of view (FOV) of approximately 202 × 202 arcsec. The clusters were centred at the reference point WFC1, located on chip 1 at position (2072, 1024). This allowed any given cluster to be observed up to a radius $r \sim 150$ arcsec from its centre, while also ensuring the cluster core did not fall near the interchip gap.

To maximize the efficiency of the limited imaging strategy afforded by a snapshot programme, all observations were made with the ACS/WFC GAIN parameter set to 2 rather than the default (GAIN = 1). This allowed the full well depth to be sampled (as opposed to only ∼75 per cent of the full well depth for GAIN = 1) with only a modest increase in read noise (∼0.3 e^- extra rms), thus increasing the dynamic range of the observations by >0.3 mag. In addition, the second image of each cluster was offset by 2 pixels in both the *x* and *y* directions, to help facilitate the removal of hot pixels and cosmic rays. With only two images per cluster, through different filters, it is not possible to completely eliminate the interchip gap using such an offset.

Before being made available for retrieval from the STScI archive, all images were passed through the standard ACS/WFC reduction pipeline. This process includes bias and dark subtractions, flat-field division, masking of known bad pixels and columns, and the calculation of photometry header keywords. In addition the STScI PYDRIZZLE software is used to correct the (significant) geometric distortion present in WFC images. The products obtained from the STScI archive are hence fully calibrated and distortion-corrected images, in units of counts per second.

The F555W images of NGC 1928, 1939 and Reticulum may be seen in Fig. 1. Both NGC 1928 and 1939 are extremely compact clusters set against heavily populated background fields, while Reticulum is at the other end of the scale – extremely diffuse with almost no background population evident. A second cluster is visible in the image of NGC 1939, slightly to the lower left of the main cluster. This is another LMC member, NGC 1938 (see Section 4.4 and Fig. 8).

For each cluster, photometry was performed on the two images individually, using the DAOPHOT software in IRAF. The detailed procedure was as follows. First the DAOFIND task was used with a detection threshold of 4σ above background to locate all the brightness peaks in each image. The two output lists were matched against each other to find objects falling at identical positions in the two frames. Objects detected in the first image but with no matching counterpart in the second image (and vice versa) were discarded.

Performing this cross-matching was not as simple a task as it might at first appear. Because of the significant geometric distortion present in the ACS/WFC observations, a 2 × 2 pixel offset in the telescope position (i.e. in the position of the object on the detector) between the two exposures does not correspond to a 2 × 2 pixel offset between the two distortion-corrected images. In fact, the value of the offset is position dependent in the corrected images. There are at least two possible ways to overcome this. The simplest is to use the header information in each of the two images to overlay a common coordinate system [e.g. J2000.0 (α, δ) coordinates] and match between the lists via a transformation from pixel coordinates to the common coordinate system. However, this procedure

Table 1. ACS/WFC observations of NGC 1928, 1939 and Reticulum (*HST* programme 9891).

Cluster	RA (J2000.0)	Dec. (J2000.0)	Filter	Data set	Exposure time (s)	Date
NGC 1928	$05^h\,20^m\,57\overset{s}{.}51$	$-69^\circ\,28'\,41\overset{''}{.}5$	F555W	j8ne62ztq	330	2003/08/23
			F814W	j8ne62zvq	200	2003/08/23
NGC 1939	$05^h\,21^m\,26\overset{s}{.}63$	$-69^\circ\,56'\,58\overset{''}{.}2$	F555W	j8ne63tqq	330	2003/07/27
			F814W	j8ne63ttq	200	2003/07/27
Reticulum	$04^h\,36^m\,09\overset{s}{.}33$	$-58^\circ\,51'\,40\overset{''}{.}3$	F555W	j8ne43a3q	330	2003/09/21
			F814W	j8ne43a7q	200	2003/09/21

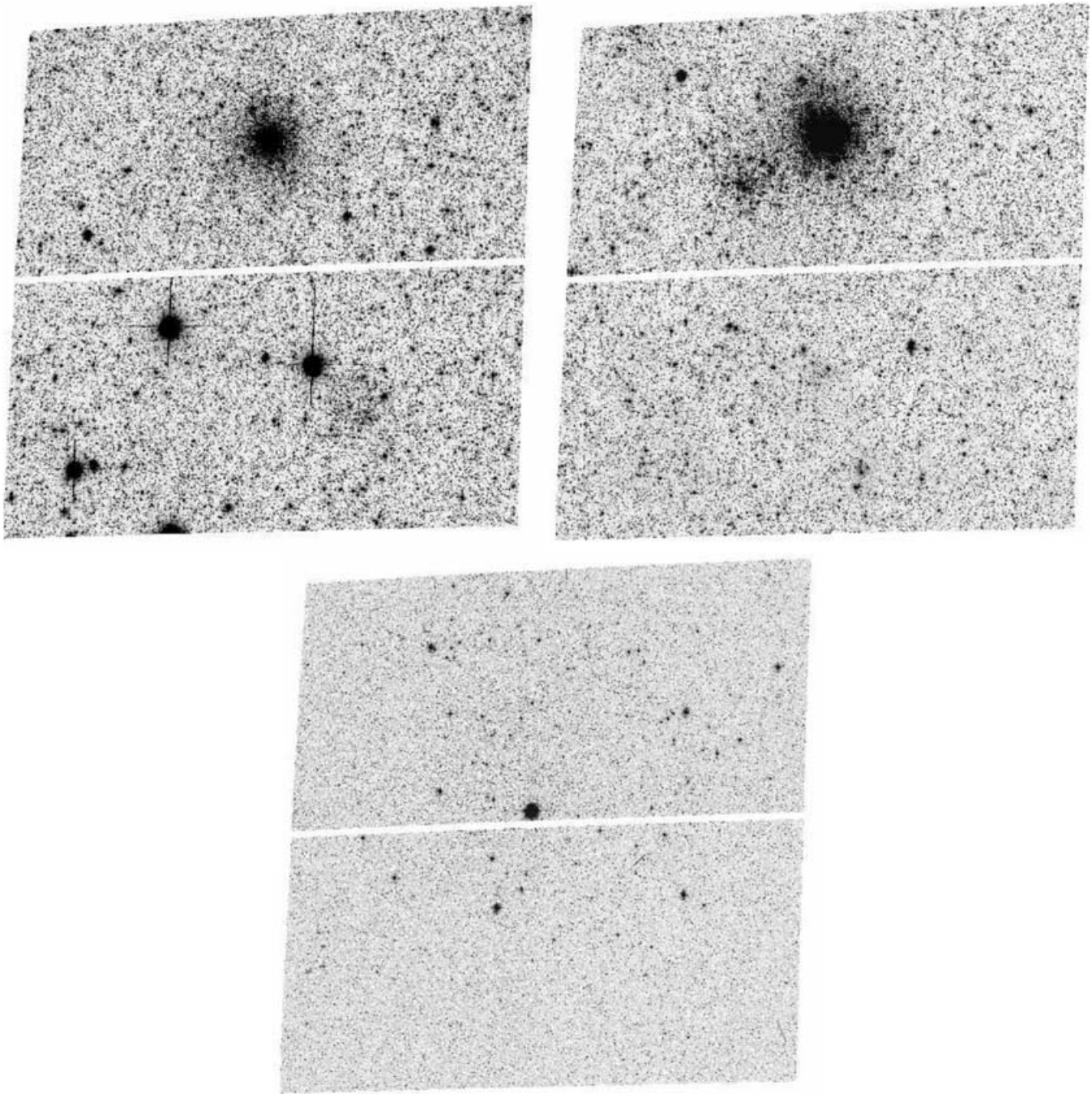

Figure 1. Distortion-corrected F555W-band ACS/WFC images of NGC 1928 (upper left), NGC 1939 (upper right) and Reticulum (lower). Note the presence of a second cluster (NGC 1938) in the NGC 1939 frame – this object lies to the lower left of the main cluster.

is completely dependent on the accuracy of the header information in each of the two data sets and the consistency between them, and we possessed no independent means of verifying this for all the observations. Instead, we preferred a more generally applicable and physically grounded procedure. We applied the distortion models used in PYDRIZZLE to transform the observed F555W positions from the distortion-corrected frame to detector positions (i.e. in the distorted frame). The new coordinates were then subjected to the 2 × 2 pixel offset and transformed into the F814W distortion-corrected frame. This allowed a direct match against the list of object positions measured by DAOFIND from this frame. Given that the distortion models are accurate to a small fraction of a pixel, a match was defined as the transformed F555W position lying within a 0.8-pixel radius of an F814W position. Experimentation showed this limiting radius to be perfectly adequate across the full WFC FOV.

The model defining the relationship between detector coordinates and distortion-corrected coordinates takes the form of a polynomial transformation

$$x_{\rm c} = \sum_{i=0}^{k} \sum_{j=0}^{i} a_{i,j} (x - x_{\rm r})^j (y - y_{\rm r})^{i-j} \quad (1)$$

$$y_c = \sum_{i=0}^{k} \sum_{j=0}^{i} b_{i,j}(x - x_r)^j (y - y_r)^{i-j} \quad (2)$$

where (x, y) are the detector coordinates (in pixels), (x_c, y_c) are the corrected coordinates (in arcsec), (x_r, y_r) is the position of a reference pixel and k is the order of the polynomial. The inverse transformation takes a similar form. Additional corrections are required to provide a grid common to the two chips which make up the WFC. Full details of the model, including its derivation and application, are provided by Mack et al. (2003). The latest solution may be downloaded from the STScI web site in the form of a matrix of the polynomial coefficients ($a_{i,j}$, etc) along with the required offsets, reference pixel values and plate scales. The version used in the present work was named nar11046j_idc.

With the cross-matching complete, lists of detected objects were provided to the PHOT task. This was used to perform aperture photometry on each object, using apertures of radius $r = 3$ pixels. We also attempted to use DAOPHOT routines to perform point spread function (PSF)-fitting photometry; however, the quality and internal consistency of the measurements we obtained was not as good as for the aperture photometry. The reasons for this likely have to do with both the nature of the images and of the objects imaged. The PSF is apparently significantly variable across the WFC FOV (possibly owing to small imperfections in the distortion correction); while the observations of NGC 1928 and 1939 are extremely crowded (we measured more than 10^5 detections in each field), meaning that it is difficult to find suitable stars to construct model PSFs across the entire FOV. The 3-pixel aperture photometry radius is large enough to be relatively insensitive to PSF variations and small enough to be usable given the crowding, so is an acceptable compromise.

The resultant photometry has been calculated in the STmag system, defined as $m = -2.5 \log_{10} f_\lambda - 21.1$, where f_λ is the flux density per unit wavelength, and the zero point is set so that Vega has magnitude 0 in the Johnson V passband. The constants required to convert the measured photometry from counts to f_λ were selected from the ACS zero-points web page, and correspond to applying the formula $m = -2.5 \log_{10}(\text{counts s}^{-1}) + ZP$, where $ZP = 25.672$ for the F555W filter and $ZP = 26.776$ for the F814W filter.

Like all previous *HST* CCD instruments, the ACS/WFC chips are suffering from degradation of their charge transfer efficiency (CTE) owing to radiation damage. As ACS is a relatively new instrument, this degradation is not yet large. None the less, photometric measurements already require correction to account for lost flux from imperfect CTE. A calibration of the losses owing to parallel (y direction) CTE effects for ACS/WFC has been provided by Riess (2003), who parametrizes the necessary correction by

$$\Delta_Y = 10^A s^B f^C \frac{Y}{2048} \frac{(\text{MJD} - 52333)}{(52714 - 52333)} \text{mag}, \quad (3)$$

where the sky (s) and flux (f) values of the object are in counts, Y represents the number of parallel transfers (so if the object has position (x , y), then $Y = y$ for $1 \leqslant y \leqslant 2048$ and $Y = 4096 - y$ for $y > 2048$) and MJD is the Modified Julian Date of the observation being corrected. The Riess calibration provides exponents $A = 0.45 \pm 0.10$, $B = -0.11 \pm 0.03$ and $C = -0.65 \pm 0.04$ for aperture photometry measurements with radius $r = 3$ pixels. At present there appear to be no additional corrections required for serial (x-direction) transfer.

With the CTE corrections calculated, the final step was to determine aperture corrections for each of the measured images. In principle it is desirable to correct to an infinite aperture; however, this was not possible here as no standard stars were observed in our images. Alternatively, it is common to correct to a set aperture, after which a transformation which includes correction to an infinite aperture is often applied to the measurements to place them on a standard magnitude scale (e.g. to move from F555W flight magnitudes to standard Johnson V magnitudes). At the time of writing, however, no such transformations are yet available for the ACS/WFC filter system. None the less, it has become common practice for WFPC2 measurements to correct to an aperture of radius 0.5 arcsec as prescribed by Holtzman et al. (1995). We therefore calculated a correction to this aperture (10 ACS/WFC pixels) for the present photometry. It is important to note that the aperture correction does not affect the relative photometry for a given cluster as it is applied uniformly across each set of measurements. It is in general important only for placing the photometry on an absolute scale. As an indication of the systematic absolute error, the energy encirclement plots provided by Mack et al. (2003) show that just under 95 per cent of the flux of a point source is contained within an 0.5-arcsec radius. Once suitable transformations for ACS/WFC photometry have been published, it will be a simple procedure to recalculate the corrections to the required aperture and convert to a standard magnitude system.

Aperture stars were selected according to strict criteria: they must be bright stars but significantly below saturation; they must not have unusual shape characteristics (see Section 3); they must have no neighbouring stars, bad pixels or image edges within a radius of 1 arcsec; and they must not lie in an area of unusually high background (e.g. near the centre of a cluster). For NGC 1928 and 1939 these criteria defined a set of several hundred stars per image, while for Reticulum the set numbered approximately 100 stars. The photometry procedure described above was repeated on these star lists using apertures of radius 10 pixels, and the mean aperture correction for each image calculated using a 3σ clipping algorithm. Standard errors in the calculated corrections were typically $\sim$0.01 mag.

3 COLOUR–MAGNITUDE DIAGRAMS

CMDs for the three clusters are presented in Fig. 2. These diagrams show all matched detections – there has been no selection of objects according to shape characteristics (see below). It is clear that the diagrams for NGC 1928 and 1939 are dominated by field stars, as expected. NGC 1928 lies against a denser field than NGC 1939. Without some form of statistical subtraction, it is impossible to determine which parts of these two CMDs belong to the clusters. The NGC 1939 field suffers in addition from severe differential reddening, as is evident from the smearing of the red clump. In contrast, the CMD for Reticulum is well defined and contains little or no field contamination. The narrowness of the sequences visible in all three CMDs (e.g. the red-giant branches) clearly demonstrate the high internal accuracy of the photometry and the validity of the reduction procedure described in the previous section.

3.1 Field star subtraction

While the CMD for Reticulum clearly possesses little or no field star contamination, statistical subtraction of the field population was absolutely necessary before any study of NGC 1928 and 1939 could be made. For such severely contaminated clusters, statistical subtraction is not a trivial matter. We developed two different subtraction methods and combined the results of each.

The first stage was to remove objects with unusual or non-stellar shape characteristics. Photometry for such objects is likely to be compromised (e.g. by a cosmic-ray strike, bad pixel or the blend of

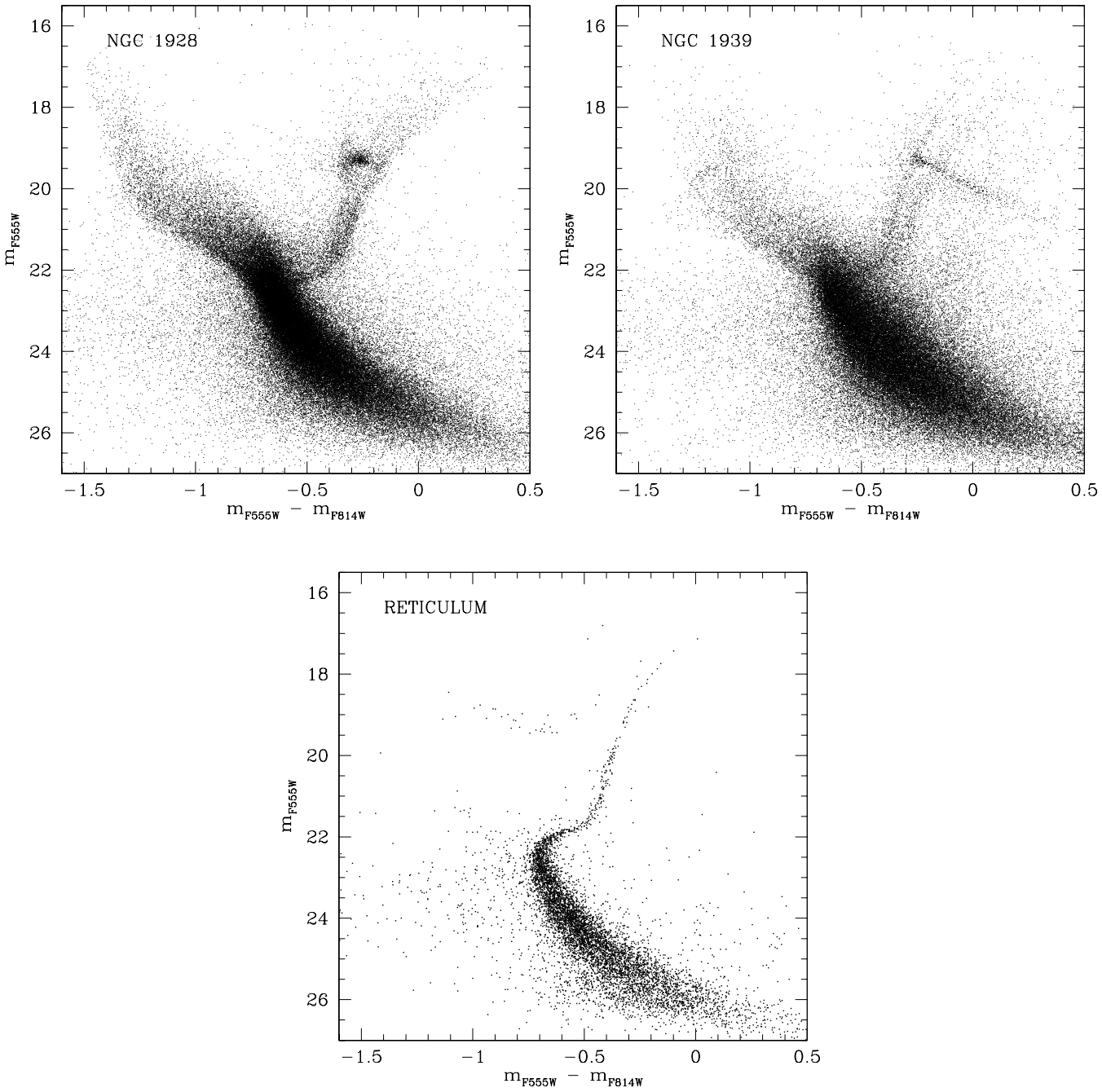

Figure 2. CMDs for all detections in each of the three fields. Measurements are plotted in the STmag magnitude system (see text). The CMD for NGC 1928 contains 104 438 detections, while that for NGC 1939 contains 94 546 detections, and the CMD for Reticulum contains 7604 detections.

two or more very close stars), or the objects are likely to be background galaxies. Either way, it is desirable to remove them from the CMDs. The output of the initial detection program, DAOFIND, provided three shape characteristics per detection: a sharpness parameter and two roundness parameters (called 's-round' and 'g-round'). The sharpness is a measurement of how high the peak of a detection is relative to a best-fitting Gaussian, while the two roundness parameters are measurements of how circular the object image is. Clean stellar detections should have sharpness ∼0.75 and round images (roundness parameters ∼0). For each photometry list we produced histograms of these three parameters to determine suitable clipping limits. In general we removed objects which did not have $0.6 <$ sharpness < 0.9 and $-0.35 <$ roundness < 0.35 through both filters. This reduced the photometry lists for NGC 1928 and 1939 by ∼35 per cent, and that for Reticulum by ∼50 per cent (although for this cluster the removed objects were almost exclusively near the faint limit of detection).

The Reticulum photometry required no further subtraction. For NGC 1928 and 1939, each photometry list was split into three groups according to radius from the centre of the cluster.[1] The aim was to

[1] We determined the two cluster centres by eye – a procedure accurate enough for present purposes given the very compact nature of both objects.

select two radii (r_1 and r_2) for each cluster, so that the detections within r_1 defined as clean a cluster sample as possible, while those outside r_2 defined a clean field sample. The sample in between r_1 and r_2 consisted of a mixed field/cluster sample. A small amount of experimentation allowed appropriate values for these radii to be chosen. To define r_1, photometry lists were assembled for all stars inside $r = 5$–25 arcsec at 1-arcsec intervals. CMDs were constructed for each of these lists, and r_1 selected to produce a well-defined CMD with as little field contamination as possible. For NGC 1928, $r_1 = 12$ arcsec, while for NGC 1939 $r_1 = 15$ arcsec. These results are consistent with the fact that NGC 1928 is more compact than NGC 1939 (see Fig. 1), as well as the fact that NGC 1928 is set against a denser field than NGC 1939 (see Fig. 2) – both of which suggest that r_1 should be smaller for NGC 1928 than NGC 1939. We note that for these measurements and all subsequent calculations, all stars within 12 arcsec of the centre of NGC 1938 on the NGC 1939 frames were excluded as a large fraction do not belong either to NGC 1939 or its background field. The characteristics of this cluster are described briefly in Section 4.4.

Selecting radius r_2 was a matter of estimating the tidal radius (r_t) for each cluster. Calculating the surface density of stars in radial bins of width 5 arcsec from 50 to 140 arcsec showed the density to be approximately constant beyond ∼90 arcsec for NGC 1928 and ∼100 arcsec for NGC 1939. These measurements are consistent with previous measurements for other compact LMC bar clusters. For example Olsen et al. (1998) constructed King models for NGC 1754, 1835, 2005 and 2019, and found $r_t \sim 115$, 85, 105 and 145 arcsec, respectively. Similarly, Mateo (1987) measured $r_t \sim$ 50, 145 and 160 arcsec for NGC 1754, 1786 and 1835, respectively. Elson & Freeman (1985) presented a high-quality surface brightness profile and King model for NGC 1835 (the most massive of the old LMC bar clusters, see Mackey & Gilmore 2003a), and measured $r_t \sim 190$ arcsec formally from the model. However, their profile (their fig. 4a) shows the surface brightness to be greater than 10 mag below the central value even by $r \sim 100$ arcsec. Hence, we set $r_2 =$ 100 arcsec for NGC 1928 and $r_2 = 110$ arcsec for NGC 1939. While these radii are likely smaller than the true tidal radii for these clusters, they were perfectly adequate for present purposes – allowing field samples of 22 000 and 17 000 stars, respectively. The field star density was found to be 1.48 arcsec^{-2} for NGC 1928 and 1.29 arcsec^{-2} for NGC 1939.

We subjected the photometry samples between r_1 and r_2 to two statistical subtraction procedures. The first involved using the central (cluster) CMD to subtract a matching CMD from the sample, leaving the field stars. The necessary number of subtractions was calculated using the measured field star density to estimate the expected total number of field stars in the region between r_1 and r_2. This in turn defined the expected number of cluster stars in the region – that is, the required number of subtractions. We did not account for detection completeness in these estimates. As regions closer in to the cluster have higher stellar densities, the detection completeness decreases with decreasing radius. The completeness is also a function of stellar magnitude and colour. Because the density of detected field stars in the region between r_1 and r_2 is, overall, less than in the outer region, assuming full completeness in this area leads to an overestimate of the number of field stars in the intermediate region and hence an underestimate of the cluster population. However, this was not a significant problem for the present work, primarily because the area suffering from the greatest incompleteness is within r_1 for both clusters. For radii greater than r_1 we estimate the completeness to be greater than 90 per cent for all areas of interest on the CMD (i.e. excluding the lower main sequences (MSs), where photometric errors are, in any case, large). In addition, our primary aim was not to obtain a subtraction of *all* possible cluster stars. Rather, we wanted to observe clean CMDs for NGC 1928 and 1939 for the first time, for the purposes of photometric study. Had we been interested in total number counts (as we would be in the construction of a brightness profile, for example) full artificial star tests would have been carried out (see Mackey & Gilmore, in preparation).

The subtraction process was as follows. First, a random star from the central region CMD was selected. On the intermediate region CMD, all non-subtracted stars within a 3σ error ellipse from this star were located, and one randomly subtracted. If there were no stars within the ellipse, the nearest neighbour was subtracted, providing it did not lie unreasonably distant from the point (i.e. not more than $\sim 6\sigma$). This process was repeated the required number of times to obtain a realization of the subtracted cluster CMD. In any such realization, multiple selections of a central region star were allowed, but a star could not be subtracted from the intermediate region more than once.

For both NGC 1928 and 1939, 100 CMD realizations were calculated. With these complete, each star in the intermediate region was checked to find how many times it had been subtracted. Stars with a large number of subtractions to their name were most likely to be cluster members. For both clusters, a histogram of this statistic was constructed, allowing a suitable cut-off to be estimated. A small amount of experimentation showed that selecting all stars with more than 75 subtractions provided clean, well-defined CMDs.

The second subtraction method was very similar, but involved using the outer (field) CMD to subtract a matching CMD from the intermediate sample, leaving the cluster stars. The required number of subtractions was again determined using the measured field star density in the outer region. As before, detection completeness was not accounted for, meaning the estimated number of field stars (and hence subtractions) was overestimated. The subtraction process was identical, except this time random stars from the outer region CMD were selected. Once again, 100 realizations of the CMD of each cluster were obtained and the stars appearing the most times in these CMDs selected as the most likely cluster members. For this method, selecting all stars with more than 50 subtractions provided good CMDs. Owing to the differential reddening present in the outer field regions of the NGC 1939 frame, this subtraction method was not as effective for this cluster. None the less, adequate results were obtained.

3.2 Final cluster CMDs

The final cleaned, field-subtracted CMDs for NGC 1928, 1939 and Reticulum appear in Fig. 3. In this figure, the CMDs for NGC 1928 and 1939 represent the combined results of the two subtraction processes. Stars within r_1 have also been plotted for both clusters, as these are very predominantly cluster members. To the best of our knowledge these are the first published CMDs for NGC 1928 and 1939. It can clearly be seen that these two clusters are very old, thus confirming the results obtained by Dutra et al. (1999) using integrated spectroscopy. Both clusters appear to possess well-populated horizontal branches (HBs), consisting almost entirely of blue stars. In this respect they strongly resemble the old LMC clusters Hodge 11 (Walker 1993; Mighell et al. 1996; Johnson et al. 1999) and NGC 2005 (Olsen et al. 1998). In addition, NGC 1928 apparently possesses an extended blue HB (BHB), falling to $V \sim 23$. The effects of differential reddening on the field subtraction for NGC 1939 can be seen in its lower MS, which exhibits a sharp cut-off to the

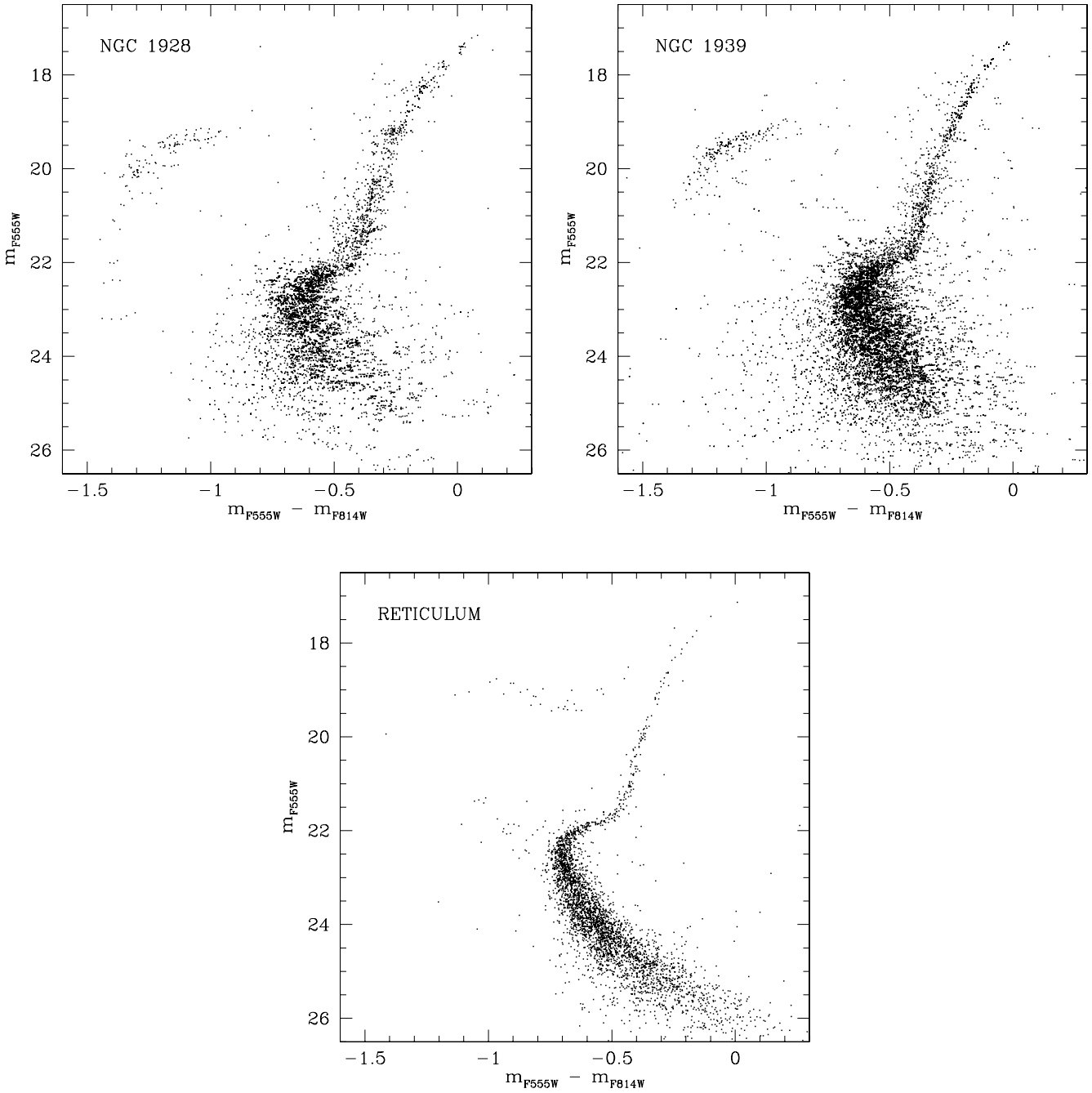

Figure 3. Cleaned, field-subtracted CMDs for the three clusters. For both NGC 1928 and 1939, the plotted points are the combined results of the two field-subtraction algorithms, along with the central sample of stars.

red. The remainder of the CMD has not been significantly affected by this problem.

Reticulum is also seen to be an old cluster, with a HB primarily consisting of stars within and to the red of the instability strip. A significant population of blue stragglers also appears to be present. This CMD confirms the earlier results of Walker (1992), Johnson et al. (2002), Marconi et al. (2002) and Monelli et al. (2003).

Ideally, we would like to use the final CMDs to provide photometric measurements of the cluster reddenings and metallicities, and to place some constraints on their ages. However, such calculations generally require the photometry to be on a standard magnitude scale – in this case, Johnson *V* and Cousins *I*. At the time of writing, no transformations from the ACS/WFC STmag system to the Johnson–Cousins *VI* system are yet available. None the less, we were able to determine an approximate transformation. One of the clusters from the present study – Reticulum – has previously been observed with *HST*/WFPC2 through the F555W and F814W filters (as part of programme 5897). Calibrations for these filters to the Johnson–Cousins *VI* system *do* exist and are well established (Holtzman et al. 1995; Dolphin 2000b). The relevant archived data groups are labelled u2xj0605b (5 × F555W frames – two with exposure durations of 260 s and three with exposure durations of 1000 s) and u2xj0608b (6× F814W frames – two with exposure durations

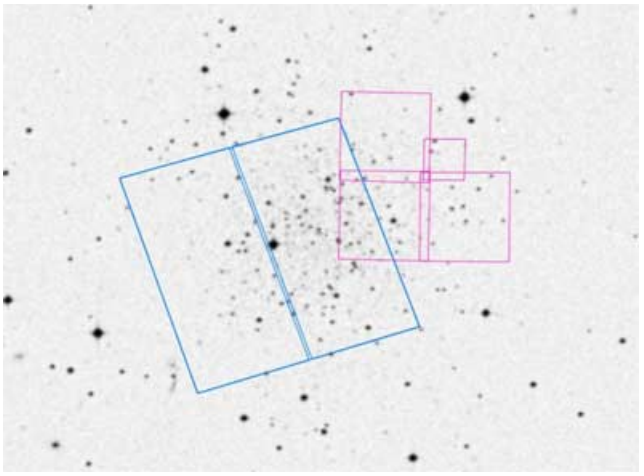

Figure 4. Position and orientation of the present ACS observations of Reticulum and the archival WFPC2 observations, superimposed on a DSS image. North is toward the top and east to the left. For some idea of the scale, the ACS FOV is approximately 202 arcsec on a side. There is a small overlap between the two sets of observations, but the bulk of the WFPC2 field lies more than 1 arcmin to the north-west of the ACS frames.

of 260 s and four with exposure durations of 1000 s). Unfortunately, these observations did not image the cluster core, but are centred ∼1.5 arcmin to the north-west. Fig. 4 shows the positions of the two observation sets overlaid on a DSS image of Reticulum. While there is a small overlap, the number of common stars was not large enough to derive a point-by-point photometric transformation. None the less, it was still possible to calculate a global transformation.

First, photometric measurements were performed on the archival WFPC2 images using HSTPHOT (Dolphin 2000a). The measurement procedure is described fully by Mackey (2004), and is identical to the procedure used by Mackey & Gilmore (2003d) to measure RR Lyrae stars in the globular clusters of the Fornax dwarf galaxy. The resultant CMD may be seen in Fig. 5.

We next determined fiducials for both the CMD from the present study (in the ACS/WFC STmag system) and the CMD from the archival WFPC2 data (in V, $V - I$). The MSs are well populated enough that the fiducials below the turn-off could be calculated by forming magnitude bins and finding the mode in colour for each. This would typically also work for the RGB, but on neither CMD is this region particularly well populated (Reticulum is a very sparse cluster). Thus, the RGB fiducials were determined by eye, as were the fiducials around the turn-off and subgiant branch (SGB). These latter could not be measured via a simple binning technique because they are neither horizontal nor vertical. As can be seen in Figs 3 and 5, the dispersion in these regions of each CMD is small (particularly for the ACS measurements), so the by-eye procedure should not introduce any large errors. This algorithm is very similar to many used in previous studies (see e.g. Johnson et al. 1999). The HB levels were determined using the (very few) stars just to the blue of the instability strip. Owing to the lack of multi-epoch observations (especially for the ACS data), the RR Lyrae regions possess a significant spread in magnitude because of the intrinsic stellar variability.

On each CMD, the colour of the MS turn-off (MSTO) was determined by fitting a second-order polynomial to the data in this region, and finding the bluest point of the fit. The magnitude of a MS reference point $V_{0.05}$ (the point on the MS which is 0.05-mag redder than the MSTO) was then determined by interpolating along

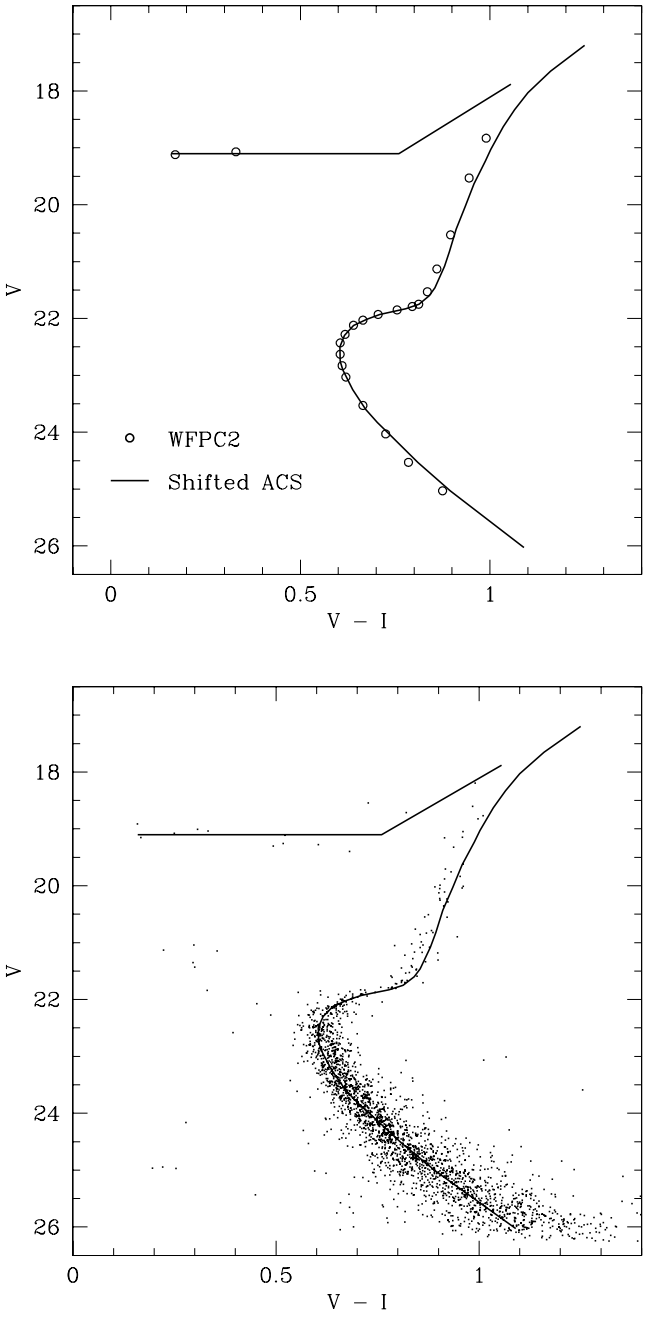

Figure 5. The shifted Reticulum fiducial as determined from ACS/WFC photometry, compared with the Reticulum fiducial from the WFPC2 photometry (upper panel) and the WFPC2 photometry itself (lower panel). The ACS/WFC fiducial has been moved 0.03-mag fainter in V and 1.31-mag redder in colour, as described in the text.

the fiducial line. These two values are traditionally used to register cluster CMDs for the purposes of differential age comparison (VandenBerg, Bolte & Stetson 1990; see Section 4.3); however, our purpose here was to determine a linear shift between the ACS/WFC photometry, and the standard Johnson–Cousins scale. By moving the ACS/WFC fiducial so that the colour of its MSTO matched that for the WFPC2 fiducial, and its $V_{0.05}$ matched that for the WFPC2 fiducial, this transformation was calculated. We found that $V - m_{\mathrm{F555W}} = 0.03$ and $(V - I) - (m_{\mathrm{F555W}} - m_{\mathrm{F814W}}) = 1.31$. The registered fiducials may be seen in the top panel of Fig. 5, while the

shifted ACS fiducial is plotted on the WFPC2 CMD in the lower panel of this figure. The registration is very close across all parts of both fiducials, except in the RGBs, which are separated slightly. The upper portion of the WFPC2 RGB is uncertain owing to a lack of stars; however, the separation persists into the lower RGB area, which is well defined for both sets of photometry. The HB levels, on the other hand, match closely. Our derived transformation implies that $I - m_{\rm F814W} = -1.28$, which matches perfectly the result of Brown et al. (2003), who found exactly this relation for a 5000-K stellar spectrum.

While it is almost certain that the true transformation is not linear [the WFPC2 transformations are parametrized by quadratic functions – see Holtzman et al. (1995)], it is clear from the good match between the two Reticulum fiducials that the present approximation is a good one, and certainly accurate enough for our purposes. It is not clear why the two RGBs show a small offset (∼0.02 mag). It is possible that this is a second-order distortion (e.g. a stretch along the colour axis). If this were the case, we would expect a similar offset between the lower MSs, which lie at approximately the same colour as the RGBs. There is indeed a hint of such an offset between the two sequences on the lower MS, although it is noted that the photometric errors are large at these faint magnitudes. We would also expect the discrepancy to become larger with redder colours, and again, while there is a hint of this on the RGBs, the upper two points on the WFPC2 fiducial are uncertain. None the less, the possibility of second-order distortions (of the order of 0.02 mag) must be considered in any calculations involving the ACS/WFC CMDs, such as those in the next section, until the full ACS/WFC calibration is complete and comprehensive transformation equations are published.

4 CLUSTER PROPERTIES

4.1 Abundances and reddenings

We employed the technique of Sarajedini (1994) to calculate photometric estimates for the reddening and metallicity of each of the three clusters. In this technique, the height of the RGB above the HB at intrinsic (dereddened) colour $(V - I)_0 = 1.2$ is used to determine the metallicity (this parameter is labelled $\Delta V_{1.2}$), while the reddening is obtained from the colour of the RGB at the level of the HB, $(V - I)_{\rm g}$. The input parameters are hence the V magnitude of the HB and some parametrization of the shape of the RGB – we chose to use the common procedure of fitting a second-order polynomial to the RGB points above the HB. This took the form $(V - I) = a_0 + a_1 V + a_2 V^2$. We fit this relation iteratively, discarding outlying points on each iteration. The results may be seen in Table 2, and graphically in Fig. 6.

Measuring accurately the level of the HB ($V_{\rm HB}$) was not a trivial procedure, especially for NGC 1928 and 1939, which have predominantly BHB morphologies, and unknown reddenings. Ideally in such cases, we would like to use the level of the reddest HB stars on the blue side of the instability strip. Using the RR Lyrae stars in four globular clusters in the Fornax dwarf spheroidal galaxy, Mackey & Gilmore (2003d) found the blue edge of the instability strip to lie at an intrinsic colour of $(V - I)_{\rm BE} = 0.28 \pm 0.02$. We employed an iterative technique to determine $V_{\rm HB}$ in conjunction with $E(V - I)$ and [Fe/H] for each cluster. We first determined estimates for $V_{\rm HB}$ using the reddest end of the populated BHB region for NGC 1928 and 1939, and the bluest HB stars for Reticulum. For a given cluster, we then solved for $E(V - I)$ and [Fe/H] following Sarajedini (1994), and used the value of $E(V - I)$ so determined to locate the HB stars just to the blue of the edge of the instability strip at $(V - I)_0 = 0.28$. These stars defined a new value for $V_{\rm HB}$, and the process was iterated until convergence. We estimated the (random) errors in these values again using the proscription of Sarajedini (1994). The accuracy with which we could measure $V_{\rm HB}$ was generally ± 0.05 mag, while that for $(V - I)_{\rm g}$ was greater – because of the narrowness of the RGB sequences and the stability of the quadratic fits – at ± 0.01 mag. 10 000 new fits per cluster were calculated, each time using a value of $V_{\rm HB}$ chosen randomly from a distribution with $\sigma = 0.05$ about the genuine measurement of $V_{\rm HB}$, and a new value of $(V - I)_{\rm g}$ selected randomly from a distribution with $\sigma = 0.01$ about the genuine measurement of $(V - I)_{\rm g}$. The standard deviations in the new sets of $E(V - I)$ and [Fe/H] defined the random errors in these quantities.

The final reddening and metallicity values are recorded in Table 2 along with the estimated errors. NGC 1939 is a metal-poor cluster ([Fe/H] = −2.10), while Reticulum is more metal rich ([Fe/H] = −1.66). In contrast, NGC 1928 is significantly more metal rich again with [Fe/H] = −1.27 – rendering it the most metal rich of the known old LMC bar clusters. Examination of the clean CMD for NGC 1928 supports this result, as there is a clear RGB luminosity function bump at approximately $V_{\rm HB}$. Such a bump is characteristic of clusters with intermediate metal abundance (see e.g. Sarajedini & Forrester 1995).

Our new results are all consistent with previous measurements and estimates, where these are available. NGC 1928 and 1939 have been poorly studied, with each possessing only one previous metallicity estimate. These are from Dutra et al. (1999) who compared their integrated spectra of NGC 1928 and 1939 to those for three Galactic globular clusters to estimate that [Fe/H] ≈ −1.2 for NGC 1928, and [Fe/H] ≈ −2.0 for NGC 1939. According to Burstein & Heiles (1982), the foreground reddening in the direction of both is $E(B - V) = 0.09$, which corresponds to $E(V - I) \approx 0.12$ (see e.g. Mackey & Gilmore 2003c). Reticulum has been more extensively studied. Walker (1992) found that [Fe/H] = −1.7 ± 0.1 by studying the RR Lyrae stars in the cluster, while Suntzeff et al. (1992) obtained a spectroscopic measurement of [Fe/H] = −1.71 ± 0.1. Both of these measurements are in excellent agreement with our photometric determination that [Fe/H] = −1.66 ± 0.12. On the reddening front, we measured $E(V - I) = 0.07 \pm 0.02$. Walker (1992) found that $E(B - V) = 0.03 \pm 0.02$ (i.e. $E(V - I) = 0.04 \pm 0.03$) but notes that the colours of his RR Lyrae sample at minimum light could imply a slightly higher reddening: $E(B - V) = 0.05 \pm 0.02$ (i.e. $E(V - I) = 0.07 \pm 0.03$). Marconi et al. (2002) suggest that the

Table 2. Results of the simultaneous determination of cluster reddenings and metallicities.

Cluster	$V_{\rm HB}$	a_0	a_1	a_2	$\Delta V_{1.2}$	[Fe/H]	$E(V - I)$
NGC 1928	19.30 ± 0.05	13.45040	−1.18991	0.02836	1.64 ± 0.15	−1.27 ± 0.14	0.08 ± 0.02
NGC 1939	19.30 ± 0.05	8.22729	−0.65527	0.01468	2.52 ± 0.20	−2.10 ± 0.19	0.16 ± 0.03
Reticulum	19.10 ± 0.05	10.56360	−0.91361	0.02161	2.05 ± 0.13	−1.66 ± 0.12	0.07 ± 0.02

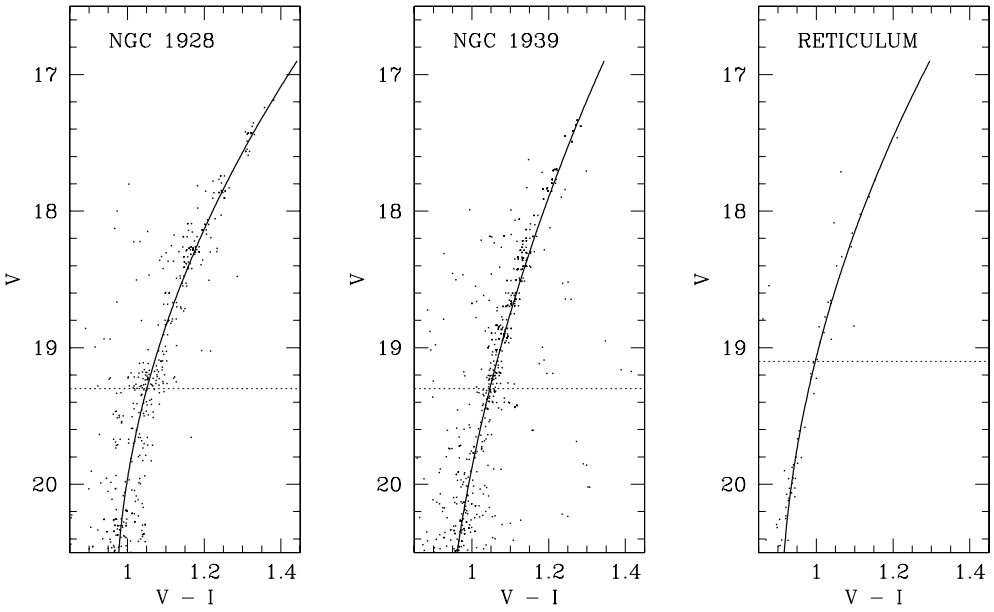

Figure 6. Quadratic fits to the three cluster RGBs, used for the reddening and metallicity determinations. The dotted lines indicate the measured HB levels.

reddening towards Reticulum could be twice as large as that suggested in the literature (i.e. $E(V-I) \sim 0.08$). All of these estimates are in good agreement with our new measurement.

As a final consistency check, if we adopt the calibration between intrinsic RR Lyrae brightness and metallicity of Chaboyer (1999),

$$M_V(\mathrm{RR}) = 0.23([\mathrm{Fe/H}] + 1.6) + 0.56, \quad (4)$$

we can calculate distance moduli (μ) for the three clusters. We find that, with $A_V = 2.37E(V-I)$ (e.g. Mackey & Gilmore 2003c), $\mu = 18.47 \pm 0.12$ for NGC 1928 and $\mu = 18.48 \pm 0.16$ for NGC 1939, where the errors represent only the effect of random measurement errors from V_{HB}, $E(V-I)$ and [Fe/H]. For Reticulum we find $\mu = 18.39 \pm 0.12$. All these estimates are in good agreement with the canonical distance to the LMC: $\mu_{\mathrm{LMC}} \approx 18.50$.

Given the uncertainties in the (approximate) photometric transformations detailed in Section 3.2, it is important to discuss briefly the potential effect of these on our metallicity and reddening measurements. The metallicity determination is obtained from a purely differential process (equation 4 in Sarajedini 1994 shows [Fe/H] to be dependent only on $\Delta V_{1.2}$) and is thus affected only by any second or higher order distortion over the range $\Delta V_{1.2}$ in V and $1.2 - (V-I)_{\mathrm{g}}$ in $V-I$. As both of these, especially the latter, are relatively small values, these distortions are unlikely to be large, and we estimate the systematic error so introduced to be less than 0.05 dex. As the distortion apparently produces an RGB which is slightly redder than appropriate (see Fig. 5), the bias is towards measurements which are too metal rich. The reddening estimates are dependent on both $(V-I)_{\mathrm{g}}$ and [Fe/H] (Sarajedini equation 3). The dependence on [Fe/H] is weak, so the primary error is introduced through $(V-I)_{\mathrm{g}}$, which could be $\sim$0.02 mag too red (see Section 3.2). This would be transferred directly to the $E(V-I)$ estimate, so it is possible these are too high by $\sim$0.02. None the less, the consistency of our estimates with both literature measurements and the LMC distance scale lead us to have confidence in the accuracy and validity of our results.

4.2 HB morphologies

Although we have images at only one epoch, and therefore no stellar variability information, it is possible to calculate a quantitative measure of the HB morphology of each cluster now that accurate reddening values are known. As part of their study of 197 RR Lyrae stars in four globular clusters belonging to the Fornax dwarf galaxy, Mackey & Gilmore (2003c) provided accurate measurements of the intrinsic $V-I$ colours of the red and blue edges of the instability strip at the level of the HB. They found $(V-I)_{\mathrm{BE}} = 0.28 \pm 0.02$ and $(V-I)_{\mathrm{RE}} = 0.59 \pm 0.02$. These values can be used to count the number of BHB stars, red HB (RHB) stars and stars on the instability strip. The HB morphology is usually parametrized by the index $(B-R)/(B+V+R)$ of Lee, Demarque & Zinn (1994), where B is the number of BHB stars, V the number of variable HB stars and R the number of RHB stars. Because we have only single epoch observations it is possible that some variables might lie outside the adopted instability strip edges (although this will not affect the morphology indices significantly, especially for NGC 1928 and 1939). In addition, because of the difficult field star subtractions necessary for NGC 1928 and 1939, our number counts are commensurately uncertain. It is none the less worthwhile to make an attempt to calculate the HB morphology for these clusters as no previous estimates exist.

For NGC 1928 we counted $R = 2^{+1}_{-2}$, $V = 3^{+1}_{-3}$ and $= 111^{+13}_{-11}$, including the putative extended BHB ($\sim$11 stars). For the more heavily populated NGC 1939 HB we counted $R = 3 \pm 3$, $V = 5^{+1}_{-5}$ and $B = 173^{+10}_{-12}$. These star counts result in a HB index of $(B-R)/(B+V+R) = 0.94^{+0.06}_{-0.04}$ for both clusters, confirming their status as having almost exclusively BHB morphologies. Reticulum clearly has a more evenly spread HB, and we count $R = 5^{+2}_{-4}$, $V = 18 \pm 3$ and $B = 5^{+0}_{-2}$, meaning a HB index of 0.00 ± 0.15. This is entirely consistent with the result of Walker (1992) who measured an index of $-0.04^{+0.00}_{-0.05}$.

4.3 Ages

While it is evident from the CMDs presented in Fig. 3 that the three clusters from the present study exhibit all the photometric qualities

of the oldest globular clusters, it is useful to obtain some quantitative measure of their ages. The best way to achieve this for the current sample is via differential comparison with clusters which have well-established ages. To this end, we employed cluster fiducials for the Galactic globular clusters M92, M3 and M5 measured by Johnson & Bolte (1998), and for the LMC globular clusters NGC 1466, 2257 and Hodge 11 measured by Johnson et al. (1999).

There is a large number of procedures available in the literature for the relative age dating of globular clusters. Perhaps the two most widely used techniques are the so-called vertical and horizontal methods. The vertical method relies on the fact that the difference between the magnitude of the MSTO and the HB is age dependent, with older clusters generally having larger values of this parameter. Similarly, the horizontal method relies on the fact that the length of the SGB is shorter for older clusters, which thus have bluer RGBs. Both techniques have a metallicity dependence which must be accounted for. We compiled metallicities from the literature for the six reference clusters. For M92, M3 and M5 these have been obtained from the data base of Harris (1996), while for NGC 1466, 2257 and Hodge 11 they are taken from various literature sources. Olszewski et al. measured spectroscopic abundances for NGC 1466 and Hodge 11 ([Fe/H] $= -2.17$ and -2.06, respectively); however, Johnson et al. (1999) suggest a slightly more metal-rich value for NGC 1466 ([Fe/H] $= -1.85$). Johnson et al. also suggest [Fe/H] $= -1.85$ is appropriate for NGC 2257 based on several previous estimates; however, Dirsch et al. (2000) obtained [Fe/H] $= -1.63$ based on a photometric study.

For NGC 1928, 1939 and Reticulum, we determined the colour and magnitude of the MSTO together with the MS reference point 0.05-mag redder than the MSTO using exactly the same technique as that described in Section 3.2. The results may be found in Table 3. These points were used for two purposes – measuring the vertical method age indicators and registering CMDs for the horizontal method (again, as described in Section 3.2). For the reference clusters, we lacked the full photometry sets, so could not apply exactly the same procedure. However, we found it perfectly adequate to fit a quadratic function to the fiducial points around the MSTO for these clusters. Johnson et al. (1999) provide measurements of $(V-I)_{\rm TO}$ and $V_{0.05}$ for NGC 1466, 2257, Hodge 11, M92 and M3. We find our calculations (again, see Table 3) to match their results very closely, which leads us to have confidence in our procedure and our measurements for M5. We estimate that our determinations of $V_{\rm TO}$ and $V_{0.05}$ are accurate to $\pm$ 0.05 mag, while those for $(V-I)_{\rm TO}$ and $(V-I)_{0.05}$ are accurate to better than $\pm$0.01 mag.

Our measured values for $\Delta V_{\rm TO}^{\rm HB}$, the difference in V between the level of the HB and the MSTO are listed in Table 3. Both of these levels are uncertain – the HB because of some intrinsic width, as well as scatter owing to stellar variability for Reticulum, and the significant weighting to the blue for NGC 1928 and 1939; and the MSTO because the MS is vertical in the turn-off region. We estimate our measurement errors in $\Delta V_{\rm TO}^{\rm HB}$ to be approximately $\pm$0.1 mag. The results in Table 3 show only a small dispersion among the clusters, even ignoring metallicity effects. Rosenberg et al. (1999) used two sets of theoretically calculated isochrones to provide a calibration for age as a function of $\Delta V_{\rm TO}^{\rm HB}$ and metallicity. This appears in their fig. 3, which shows the significant majority of the 34 Galactic globular clusters in their sample to lie within a narrow band of $\sim$2-Gyr width about mean values of 14.3 and 14.9 Gyr for the two isochrone sets. Placing our clusters on this diagram (using the metallicities listed in Table 4) shows NGC 1928 and Reticulum to lie within this band, along with all the reference clusters except Hodge 11. This cluster, along with NGC 1939 fall $\sim$2 Gyr older than the upper limit of the Rosenberg et al. 2-Gyr band.

To combat the uncertainty in $\Delta V_{\rm TO}^{\rm HB}$ introduced by measuring $V_{\rm TO}$, Buonanno et al. (1998) introduced a calibration for a similar vertical parameter, $\Delta V_{0.05}^{\rm HB}$ – the difference in V between the level of the HB and $V_{0.05}$. Because the MS is sloped at $V_{0.05}$, this measurement is in theory more accurate (although formally, our errors are the same).

Table 3. Results of the CMD registration and relative age dating measurements (vertical technique).

Cluster	$(V-I)_{\rm TO}$	$V_{\rm TO}$	$(V-I)_{0.05}$	$V_{0.05}$	$V_{\rm HB}$	$\Delta V_{\rm TO}^{\rm HB}$	$\Delta V_{0.05}^{\rm HB}$
NGC 1928	0.674	22.851	0.724	23.85	19.30	3.55	4.55
NGC 1939	0.660	22.910	0.710	23.69	19.30	3.61	4.39
Reticulum	0.603	22.627	0.653	23.41	19.10	3.53	4.31
M92	0.558	18.712	0.608	19.49	15.18	3.53	4.31
M3	0.595	19.173	0.645	19.98	15.75	3.42	4.23
M5	0.629	18.590	0.679	19.44	15.18	3.41	4.26
NGC 1466	0.622	22.860	0.672	23.73	19.32	3.54	4.41
NGC 2257	0.612	22.530	0.662	23.40	19.10	3.43	4.30
Hodge 11	0.628	22.812	0.678	23.58	19.11	3.70	4.47

Table 4. Results of the relative age dating measurements (horizontal technique).

Cluster name	[Fe/H]	$\delta_{2.5}$	Reference cluster	[Fe/H]	$\delta_{2.5}$	$\delta(V-I)$	$\Delta\tau$ (Gyr)
NGC 1928	-1.27	0.285	M5	-1.27	0.281	0.003	-0.2
NGC 1939	-2.10	0.293	M92	-2.28	0.283	0.013	-1.3
			NGC 1466	-2.17	0.289	0.006	-0.5
				(-1.85)			($+0.6$)
			Hodge 11	-2.06	0.276	0.021	-0.9
Reticulum	-1.66	0.309	M3	-1.54	0.275	0.038	-1.4
			NGC 2257	-1.63	0.290	0.023	-1.0
				(-1.85)			(-1.8)

We therefore calculated $\Delta V_{0.05}^{\rm HB}$ for each cluster for comparison with the Buonanno et al. calibration. These measurements are also listed in Table 3. The relevant calibration appears in figs 7(a)–(c) of Buonanno et al., for three isochrone sets. We note that this calibration is based on $(V\,, B-V)$ CMDs, however, it should provide some indication of age homogeneity or otherwise in our cluster sample. Plotting the clusters on this figure again shows them to lie within a band of width ∼2 Gyr, along with 14 Galactic globular clusters from the Buonanno et al. sample. The one outlier in our sample is NGC 1928, which lies ∼2-Gyr older than the band. For the three isochrone sets, the best-fitting mean ages are 14, 12 and 15 Gyr, respectively.

Rosenberg et al. (1999) provide a calibration for a horizontal dating method in addition to their vertical method calibration. The relevant parameter in this case is $\delta_{2.5}$, the difference in $V-I$ between the MSTO and a point on the RGB 2.5-mag brighter than the MSTO. Our measurements of this parameter for all the clusters are listed in Table 4. Again, these results show a good deal of internal consistency, suggesting small relative age differences. This is confirmed by consideration of fig. 4 in Rosenberg et al. which shows their age calibration including metallicity effects, again for two isochrone sets. As for the vertical age indicator, the $\delta_{2.5}$ values place all the present LMC and reference clusters within the same 2-Gyr wide band. On this occasion, there are no significant outliers.

Finally, we obtained a more quantitative measure of the relative cluster ages using the horizontal method calibration of Johnson et al. (1999). For this process, we first registered two cluster CMDs using $(V-I)_{\rm TO}$ and $V_{0.05}$, and then calculated the mean difference in colour between their RGBs from the base to the HB, $\delta(V-I)$. This was achieved using the procedure of Johnson et al. (1999). A straight line was fitted to the RGB section for the reference cluster, and then the weighted average of the difference in colour between this line and the RGB stars for relevant the LMC cluster. As $\delta(V-I)$ is sensitive to both age and metallicity, it was important to choose a reference cluster with similar metallicity to the LMC cluster under consideration. With the available clusters we had the following six matches: NGC 1928 and M5; NGC 1939 and M92, NGC 1466, and Hodge 11; Reticulum and M3, and NGC 2257. The results of the $\delta(V-I)$ calculations are listed in Table 4, while Fig. 7 shows the reference cluster fiducials registered to the relevant LMC cluster fiducials. It is immediately clear from these plots that there cannot be a large age difference between the present three clusters and the oldest Galactic and LMC globular clusters. To quantify this, we use the results of Johnson et al. (1999) who provide relations between $\delta(V-I)$, age and metallicity using two theoretical isochrone sets. The differences in the two calibrations are not large and we adopt a mean relation. First we correct $\delta(V-I)$ between an LMC cluster and a reference cluster for metallicity effects using

$$\delta(V-I) = -0.0745(\Delta[{\rm Fe/H}]) \qquad (5)$$

and then estimate the age difference using

$$\delta(V-I) = -0.0205(\Delta\tau), \qquad (6)$$

where τ represents age in Gyr. Strictly speaking this calibration is only valid over the metallicity range $-2.26 < [{\rm Fe/H}] < -1.66$; however, it is unlikely that extrapolating slightly to $[{\rm Fe/H}] \sim -1.3$ for NGC 1928 and M5 will introduce a large error. The results of the calculations are listed in Table 4. The two reference clusters NGC 1466 and 2257 have differing metallicities listed in the literature, as discussed earlier. Hence, these two clusters have a relative age range, as listed in Table 4.

None of the present three LMC clusters is more than ∼1.5 Gyr younger than any reference cluster. This offers quantitative evidence that NGC 1928, 1939 and Reticulum are true members of the oldest population of LMC star clusters, and are coeval with the oldest Galactic globular clusters. Supporting evidence is provided by the more qualitative measures offered by the vertical dating technique – the results of which are fully consistent with all the clusters being coeval to within ±1 Gyr or so. We note that it is possible that our approximate transformation to Johnson V and Cousins I photometry has introduced some systematic error into the relative age measurements – after all, we noted earlier that the transformed RGBs are possibly too red by ∼0.02 mag. In this context, it is interesting to note that all the $\delta(V-I)$ values are positive, indicating LMC cluster RGBs lying to the red of the reference cluster RGBs. This potential systematic error does not affect our conclusion, however, because redder RGBs indicate more youthful clusters. Thus, the $\Delta\tau$ values listed in Table 4 represent the maximum age differences implied by the $\delta\,(V-I)$ dating technique if the transformation is imperfect in the manner suspected – in reality it is likely that the clusters are even closer in age.

4.4 NGC 1938

It is worth plotting the CMD for the stars within 12 arcsec of the centre of NGC 1938 – which were removed from the calculations for NGC 1939 (see Section 3.1) – because we could not find any previously published CMDs for this cluster. Fig. 8 shows a close-up of the ACS/WFC F555W observation in the vicinity of NGC 1938 and 1939, with the extraction radius shown. The resultant CMD for NGC 1938 is plotted in Fig. 9. No attempt has been made to remove the field star contamination or the contamination from NGC 1939, the giant branch of which is visible. None the less, a narrow MS is clearly evident in this CMD. It is not immediately obvious that this should be associated with NGC 1938 as it is clear from Fig. 2 that it lies in the vicinity of the 'young' MS of the field population. To investigate this we calculated a crude fiducial for the sequence in Fig. 9 above $m_{\rm F555W} = 22$. We then counted all the stars less than 0.15 mag perpendicular distance from this fiducial in two bins – an upper bin ($17 \leqslant m_{\rm F555W} \leqslant 20$) and a lower bin ($20 \leqslant m_{\rm F555W} \leqslant 22$). Next, two field extractions of equivalent area to the NGC 1938 extraction (i.e. with radius 12 arcsec) were made away from both NGC 1938 and 1939 – one at 40 arcsec to the north-west of NGC 1938, and one at 1 arcmin to the north-east of NGC 1938. These were far enough away not to be contaminated by NGC 1938 or NGC 1939, and close enough not to be affected by serious differential reddening. We then repeated our star counts in these two extractions. In the on-cluster extraction we counted 64 stars in our upper bin and 107 in our lower bin. For the two off-cluster extractions we counted five and eight stars, respectively, for the upper bin, and 31 and 33 stars, respectively, for the lower bin. The star counts are clearly significantly enhanced for the on-cluster field, especially for the upper MS region. This allows us to confidently associate the sequence observed in Fig. 9 with NGC 1938 and not the general field population.

No turn-off is observed on this sequence to $m_{\rm F555W} \approx V \approx 18$. We use this fact to place an upper limit on the age of NGC 1938. Kerber et al. (2002) provide a CMD for the rich LMC cluster NGC 1831 from WFPC2 observations, which shows the turn-off to be just below $V \approx 18$. Their age estimate for this cluster is $\tau \approx 500$ Myr. Elson & Fall (1988) provide an age calibration for a large number of LMC clusters. Their age estimate for NGC 1831, corrected to a distance modulus of 18.5 is ∼300 Myr. Together these age estimates provide us with an approximate upper limit for the age of NGC 1938 of

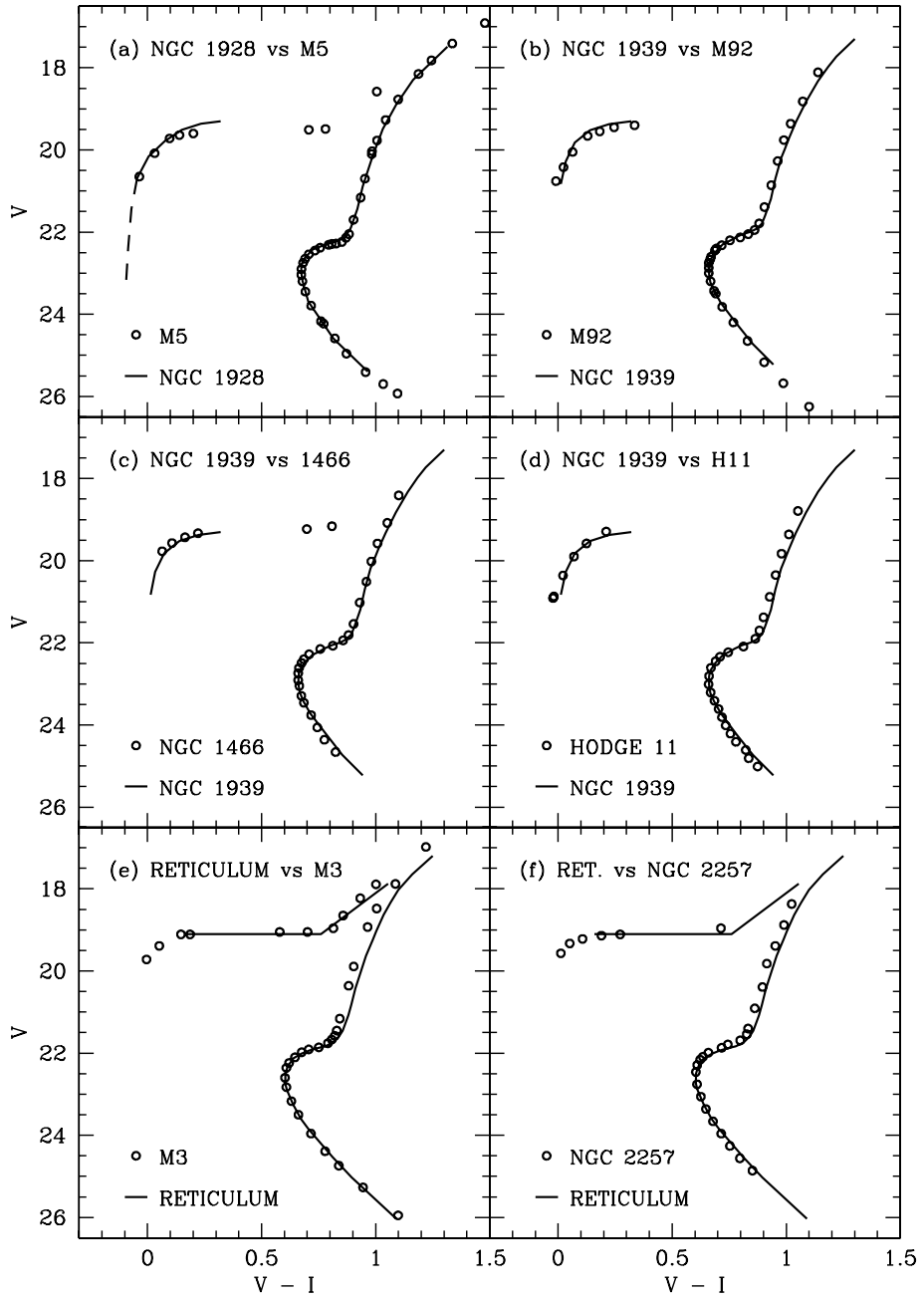

Figure 7. Reference cluster fiducials (open circles) registered to the fiducials for NGC 1928, 1939 and Reticulum (solid lines) using $(V-I)_{\rm TO}$ and $V_{0.05}$.

∼400 Myr. This result is perfectly consistent with the integrated *UBV* photometry of Bica et al. (1996), which places NGC 1938 in SWB class IVA (where the SWB class refers to the classification of Searle, Wilkinson & Bagnuolo 1980). This class brackets the age range 200–400 Myr. Owing to the very large age difference between NGC 1938 and 1939, it seems unlikely that these two clusters are physically related – rather, their apparent close proximity is merely a projection effect.

5 SUMMARY

We have used ACS/WFC snapshot observations to obtain CMDs for the LMC clusters NGC 1928, 1939 and Reticulum. This is the first time that CMDs for NGC 1928 and 1939 have been published. These two CMDs suffer from very dense field star contamination requiring a thorough subtraction algorithm. Using the final CMDs we obtained photometric reddening and metallicity measurements for all three clusters. NGC 1939 is one of the most metal-poor LMC bar clusters, with [Fe/H] $= -2.10 \pm 0.19$, while NGC 1928 is significantly more metal rich, with [Fe/H] $= -1.27 \pm 0.14$. Reticulum is of a more intermediate abundance, with [Fe/H] $= -1.66 \pm 0.12$. This measurement matches well the previous estimates for this cluster.

All three clusters possess CMDs with features characteristic of the oldest Galactic globular clusters – MSTOs at $V \sim 23$, and well-populated HBs. Both NGC 1928 and 1939 possess very blue HB morphologies, with little or no population stretching to the red of the blue edge of the instability strip. In contrast, Reticulum has a HB populated right across the instability region. To quantify the ages of

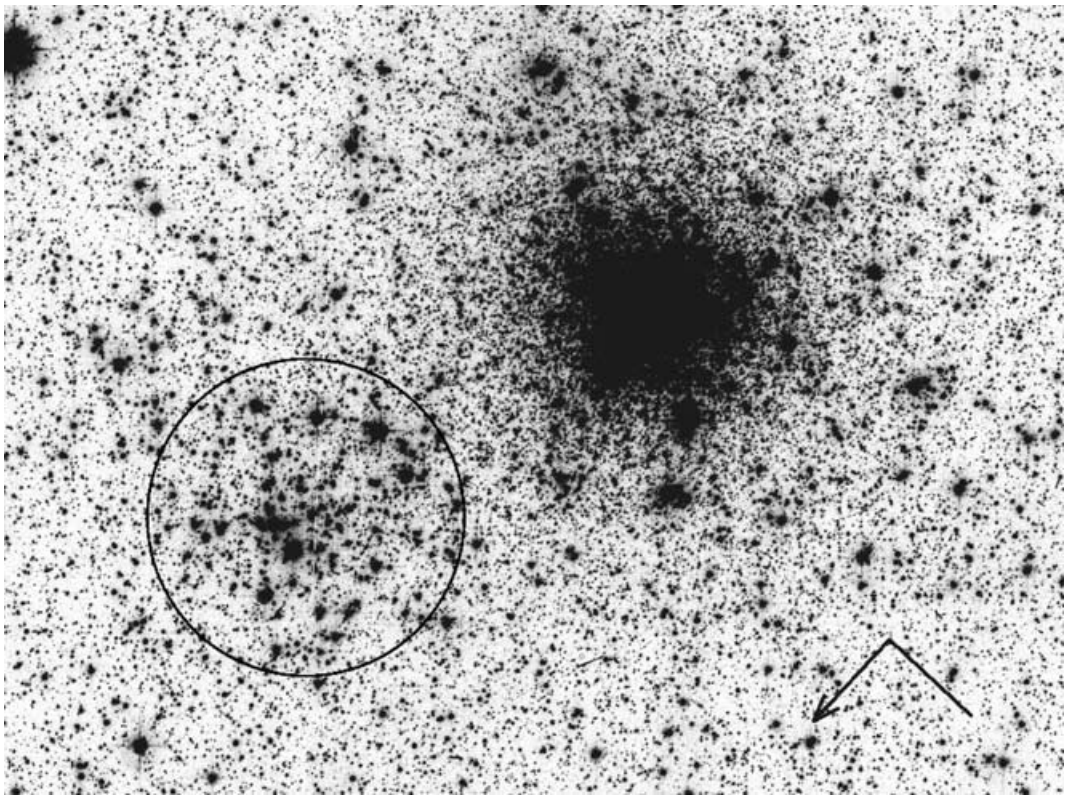

Figure 8. ACS/WFC F555W image of the region surrounding NGC 1939 and 1938 (circled). North and east are indicated (north is in the direction of the arrow). The NGC 1938 extraction radius is ∼12 arcsec.

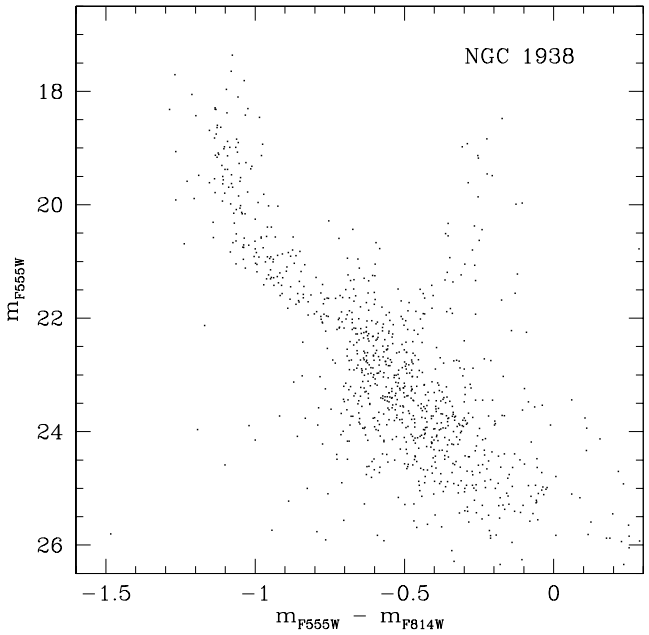

Figure 9. CMD for all stars within the 12-arcsec extraction radius around NGC 1938. As previously, measurements are in the ACS/WFC STmag system.

the three clusters we employed a variety of differential dating techniques, comparing their CMDs to a set of three of the oldest Galactic globular clusters, and three of the oldest LMC globular clusters. We conclude that the entire set of clusters is coeval to within approximately 2 Gyr. This work firmly establishes NGC 1928 and 1939 as members of the LMC globular cluster population, confirming the conclusion obtained by Dutra et al. (1999) from integrated spectroscopy. The LMC globular cluster census therefore now numbers 15, in two distinct groups – the outer clusters NGC 1466, 1841, 2210, 2257, Hodge 11 and Reticulum; and the inner (bar) clusters NGC 1754, 1786, 1835, 1898, 1916, 1928, 1939, 2005 and 2019. The only other LMC cluster older than the lower end of the age gap is ESO121−SC03, at ∼9 Gyr.

ACKNOWLEDGMENTS

This paper is based on observations made with the NASA/ESA *Hubble Space Telescope*, obtained at the Space Telescope Science Institute, which is operated by the Association of Universities for Research in Astronomy, Inc., under NASA contract No. NAS 5-26555. These observations are associated with programme 9891. ADM is grateful for financial support from PPARC in the form of a Postdoctoral Fellowship.

REFERENCES

Bica E., Clariá J. J., Dottori H., Santos J. F. C. Jr, Piatti A. E., 1996, ApJS, 102, 57

Brocato E., Castellani V., Ferraro F. R., Piersimoni A. M., Testa V., 1996, MNRAS, 282, 614

Brown T. M., Ferguson H. C., Smith E., Kimble R. A., Sweigart A. V., Renzini A., Rich R. M., VandenBerg D. A., 2003, ApJ, 592, L17

Buonanno R., Corsi C. E., Pulone L., Fusi Pecci F., Bellazzini M., 1998, A&A, 333, 505

Burstein D., Heiles C., 1982, AJ, 87, 1165

Chaboyer B., 1999, in Heck A., Caputo F., eds, Post-*Hipparcos* Cosmic Candles. Kluwer, Dordrecht, p. 111
Dirsch B., Richtler T., Gieren W. P., Hilker M., 2000, A&A, 360, 133
Dolphin A. E., 2000a, PASP, 112, 1383
Dolphin A. E., 2000b, PASP, 112, 1397
Dutra C. M., Bica E., Clariá J. J., Piatti A. E., 1999, MNRAS, 305, 373
Elson R. A. W., Freeman K. C., 1985, ApJ, 288, 521
Elson R. A. W., Fall S. M., 1988, AJ, 96, 1383
Geisler D., Bica E., Dottori H., Clariá J. J., Piatti A. E., Santos J. F. C. Jr, 1997, AJ, 114, 1920
Harris W. E., 1996, AJ, 112, 1487
Holtzman J., Burrows C. J., Casertano S., Hester J. J., Trauger J. T., Watson A. M., Worthey G., 1995, PASP, 107, 1065
Johnson J. A., Bolte M., 1998, AJ, 115, 693
Johnson J. A., Bolte M., Stetson P. B., Hesser J. E., Somerville R. S., 1999, ApJ, 527, 199
Johnson J. A., Bolte M., Stetson P. B., Hesser J. E., 2002, in Geisler D., Grebel E. K., Minniti D., eds, Proc. IAU Symp. 207, Extragalactic Star Clusters. Astron. Soc. Pac., San Francisco, p. 190
Kerber L. O., Santiago B. X., Castro R., Valls-Gabaud D., 2002, A&A, 390, 121
Lee Y.-W., Demarque P., Zinn R., 1994, ApJ, 423, 248
Mack J., Gillilan R., eds, 2003, ACS Data Handbook, Version 2.0. STScI, Baltimore
Mackey A. D., Gilmore G. F., 2003a, MNRAS, 338, 85
Mackey A. D., Gilmore G. F., 2003b, MNRAS, 338, 120
Mackey A. D., Gilmore G. F., 2003c, MNRAS, 340, 175
Mackey A. D., Gilmore G. F., 2003d, MNRAS, 343, 747
Mackey A. D., 2004, PhD thesis, Univ. Cambridge
Marconi G., Ripepi V., Andreuzzi G., Bono G., Buonanno R., Cassisi S., 2002, in Geisler D., Grebel E. K., Minniti D., eds, Proc. IAU Symp. 207, Extragalactic Star Clusters. Astron. Soc. Pac., San Francisco, p. 193
Mateo M., 1987, ApJ, 323, L41
Mighell K. J., Rich R. M., Shara M., Fall S. M., 1996, AJ, 111, 2314
Monelli M. et al., 2003, in Piotto G., Meylan G., Djorgovski S. G., Riello M., eds, ASP Conf. Ser. Vol. 296, New Horizons in Globular Cluster Astronomy. Astron. Soc. Pac., San Francisco, p. 388
Olsen K. A. G., Hodge P. W., Mateo M., Olszewski E. W., Schommer R. A., Suntzeff N. B., Walker A. R., 1998, MNRAS, 300, 665
Riess A., 2003, ACS Instrument Science Report, 2003-009
Rosenberg A., Saviane I., Piotto G., Aparicio A., 1999, AJ, 118, 2306
Sarajedini A., 1994, AJ, 107, 618
Sarajedini A., Forrester W. L., 1995, AJ, 109, 1112
Searle L., Wilkinson A., Bagnuolo W., 1980, ApJ, 239, 803
Suntzeff N. B., Schommer R. A., Olszewski E. W., Walker A. R., 1992, AJ, 104, 1743
VandenBerg D. A., Bolte M., Stetson P. B., 1990, AJ, 100, 445
Walker A. R., 1992, AJ, 103, 1166
Walker A. R., 1993, AJ, 106, 999

This paper has been typeset from a TEX/LATEX file prepared by the author.